RESEARCH/REVIEW ARTICLE

Nitrate stable isotopes and major ions in snow and ice samples from four Svalbard sites

Carmen P. Vega,[1] Mats P. Björkman,[2] Veijo A. Pohjola,[1] Elisabeth Isaksson,[3] Rickard Pettersson,[1] Tõnu Martma,[4] Alina Marca[5] & Jan Kaiser[5]

[1] Department of Earth Sciences, Uppsala University, Villavägen 16, SE-76236 Uppsala, Sweden
[2] Department of Earth Sciences, University of Gothenburg, P.O. Box 460, SE-40530 Göteborg, Sweden
[3] Norwegian Polar Institute, Fram Centre, P.O. Box 6606 Langnes, NO-9296 Tromsø, Norway
[4] Institute of Geology, Tallinn University of Technology, Ehitajate tee 5, EE-19086 Tallinn, Estonia
[5] Centre for Ocean and Atmospheric Sciences, School of Environmental Sciences, University of East Anglia, Norwich NR4 7TJ, UK

Keywords
Nitrate; isotopes; ice cores; Svalbard; pollutants.

Correspondence
Carmen P. Vega, Department of Earth Sciences, Uppsala University, Villavägen 16, SE-76 236 Uppsala, Sweden.
E-mail: carmen.vega@geo.uu.se

Abstract

Increasing reactive nitrogen (N_r) deposition in the Arctic may adversely impact N-limited ecosystems. To investigate atmospheric transport of N_r to Svalbard, Norwegian Arctic, snow and firn samples were collected from glaciers and analysed to define spatial and temporal variations (1–10 years) in major ion concentrations and the stable isotope composition ($\delta^{15}N$ and $\delta^{18}O$) of nitrate (NO_3^-) across the archipelago. The $\delta^{15}N_{NO_3^-}$ and $\delta^{18}O_{NO_3^-}$ averaged −4‰ and 67‰ in seasonal snow (2010–11) and −9‰ and 74‰ in firn accumulated over the decade 2001–2011. East–west zonal gradients were observed across the archipelago for some major ions (non-sea salt sulphate and magnesium) and also for $\delta^{15}N_{NO_3^-}$ and $\delta^{18}O_{NO_3^-}$ in snow, which suggests a different origin for air masses arriving in different sectors of Svalbard. We propose that snowfall associated with long-distance air mass transport over the Arctic Ocean inherits relatively low $\delta^{15}N_{NO_3^-}$ due to in-transport N isotope fractionation. In contrast, faster air mass transport from the north-west Atlantic or northern Europe results in snowfall with higher $\delta^{15}N_{NO_3^-}$ because in-transport fractionation of N is then time-limited.

To access the supplementary material for this article, please see supplementary files under Article Tools online.

Growing food and energy consumption has increased the amount of reactive nitrogen (N_r) released to the atmosphere over the last century (Mosier et al. 2002). This N_r can be transported to high latitudes and deposited by both dry (turbulence transfer and sedimentation) and wet deposition (rain or snow). In polar regions, N_r can be deposited with snow, stored in glaciers and released by melting of seasonal snowpacks and glacier ice (Brimblecombe et al. 1985; Björkman et al. 2014). The Arctic comprises fragile N-limited ecosystems that can be profoundly affected by even small increases of N_r inputs (Shaver & Chapin 1980; Atkin 1996; Aanes et al. 2000; Dickson 2000; Rinnan et al. 2007).

An important fraction of N_r consists of atmospheric N oxides (NO_x: $NO+NO_2$), but measuring these gases in polar regions is difficult (Bottenheim et al. 1986; Carroll & Thompson 1995). NO_x are oxidized in the atmosphere to nitrate (NO_3^-), which is one of the major ions found in polar snow. Ice-core records of NO_3^- have accordingly been used to infer past changes in atmospheric NO_x concentrations (Wolff 1995; Kekonen et al. 2002; Samyn et al. 2012). In Svalbard, Norwegian Arctic, ice cores show NO_3^- concentrations rising in the 1950s, peaking in the 1970s and decreasing after the 1980s (Goto-Azuma & Koerner 2001; Kekonen et al. 2002; Samyn et al. 2012). A 20-year record of NO_3^- deposition in precipitation from

Citation: *Polar Research* 2015, *34*, 23246, http://dx.doi.org/10.3402/polar.v34.23246

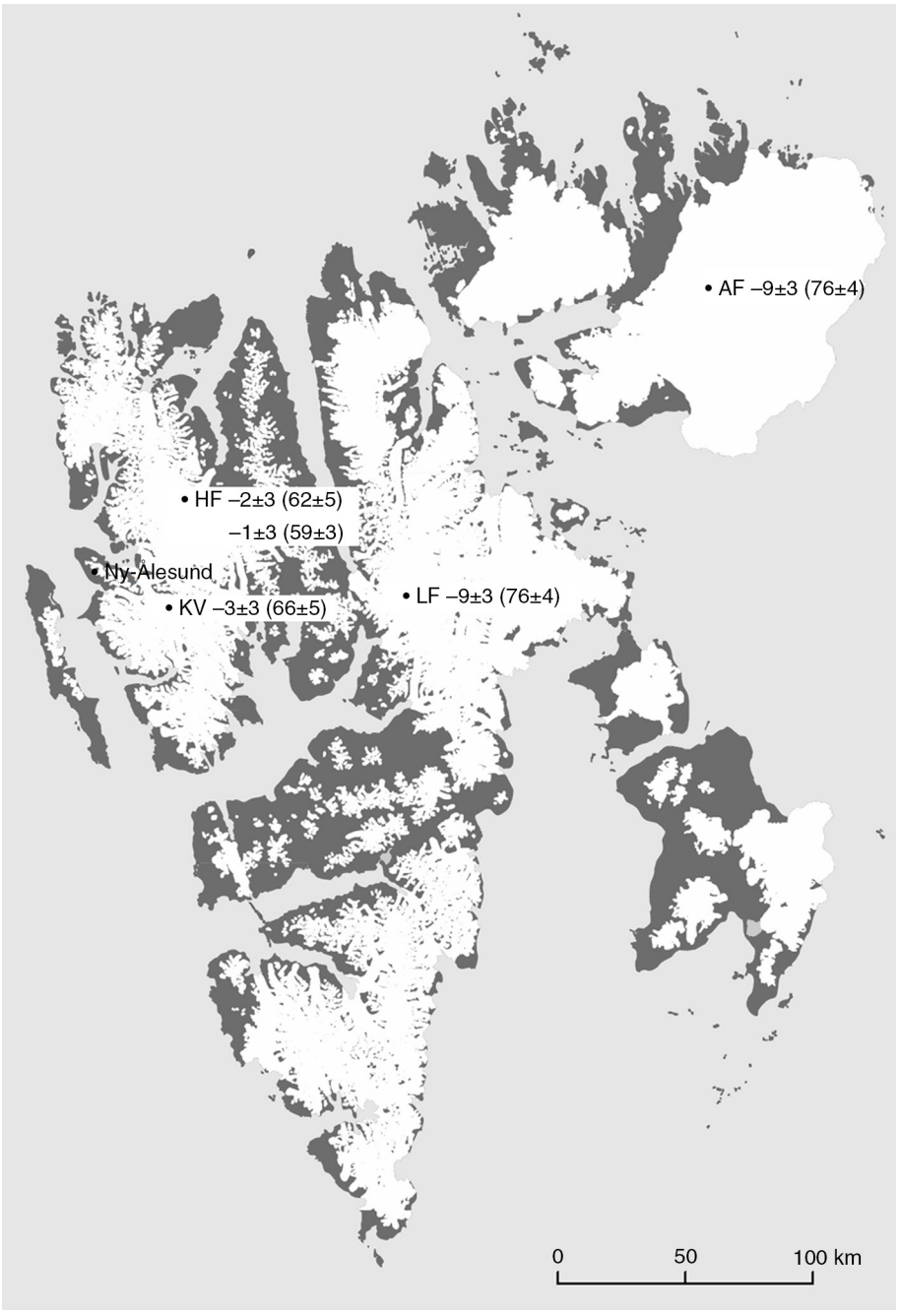

Fig. 1 Snow and firn sampling sites in Svalbard: Holtedahlfonna (HF); Kongsvegen (KV); Lomonosovfonna (LF); and Austfonna (AF). The means $\delta^{15}N_{NO_3^-}$ and $\delta^{18}O_{NO_3^-}$ (bracketed) measured in snow in this paper are shown for each site ($\pm 1\sigma$; units of ‰). Shaded relief map from the Advanced Spaceborne Thermal Emission and Reflection Radiometer (ASTER) global digital elevation model; glacier outlines from Nuth et al. (2013).

Ny-Ålesund, Spitsbergen (Fig. 1) shows that 10% of all precipitation events account for the total annual N_r deposition to the area (Kühnel et al. 2011). These events occur when blocking high-pressure systems over Scandinavia promote transport of pollution from Europe and humidity from the Atlantic (Kühnel et al. 2013).

Previous studies have shown that the stable isotope ratio $^{15}N/^{14}N$ of NO_3^- can be used to identify precursor

Citation: *Polar Research* 2015, *34*, 23246, http://dx.doi.org/10.3402/polar.v34.23246

NO_x sources in polar regions (Freyer et al. 1996; Hastings et al. 2004; Heaton et al. 2004; Hastings et al. 2009; Morin et al. 2009; Björkman 2013). In addition, the stable isotope ratio $^{18}O/^{16}O$ in the same molecule is an indicator of seasonal variations in atmospheric NO_3^- formation pathways, particularly at Arctic sites (Michalski et al. 2003; Morin et al. 2008). After deposition, NO_x can be re-emitted from snow due to photolysis of NO_3^- by sunlight (Honrath et al. 1999; Honrath et al. 2000; Dibb et al. 2002; Hastings et al. 2004; Jarvis et al. 2008). Sublimation of HNO_3 can also take place at the snow/air interface (Honrath et al. 1999; Dibb et al. 2002; Röthlisberger et al. 2002), and both photolysis and sublimation modify the $^{15}N/^{14}N$ ratio of NO_3^- in snow (Blunier et al. 2005).

The Svalbard Archipelago (Fig. 1) is the site of frequent exchange between air masses from low and high latitudes (Hisdal 1998). South-westerly transport of mild oceanic air, associated with a low-pressure system east of Iceland, often brings mild winter temperatures to Svalbard compared to other Arctic locations. In contrast, Arctic air intrusions from the north-east, driven by a high-pressure system over Greenland, can bring much colder winter temperatures. The interplay between these synoptic situations frequently creates unstable weather conditions in Svalbard, especially during winter, but also favours the long-range transport of aerosols to the archipelago, including pollutants, from continental sources to the south and east.

In this work, we report new measurements of stable isotope ratios of $^{15}N/^{14}N$ and $^{18}O/^{16}O$ in NO_3^- from firn cores and snow samples obtained at four sites in central and north-east Svalbard (Fig. 1). These new data help to better define the spatial and temporal variability of NO_3^- isotopic signatures across Svalbard by complementing previous measurements from the atmosphere and snow made near Ny-Ålesund (Heaton et al. 2004; Morin et al. 2009; Morin et al. 2012; Björkman 2013). We also present back-trajectory analyses of air masses associated with precipitation events at the different sampling sites to help identify NO_3^- source regions for this sector of the Arctic.

Methods

Lomonosovfonna and Austfonna firn cores

An 8.0-m-long firn core (LF-11) was drilled at the summit of the Lomonosovfonna icefield in central Spitsbergen in April 2011 (Fig. 1, Table 1). A Kovacs drill with an internal diameter of 8.5 cm and a barrel length of 1.6 m was employed. The core was packed in clean plastic sleeves and stored at −20°C during transport between Svalbard and Tromsø, Norway, where the core was sampled at the facilities of the Norwegian Polar Institute (NPI). Clean protocols were employed when cutting and sampling the core (for details see Vega et al. 2015). The ice core was divided into three pieces with 1.8 cm × 1.8 cm square cross sections, which were then cut in samples of 4 cm length each, for analyses of water stable isotope ratios ($^{18}O/^{16}O$), major ion and black carbon (BC) (the BC data will be reported elsewhere). The remaining sections (1.8 cm × 3.6 cm × ca. 70 cm) were used for stable isotope ratio measurements of $^{15}N/^{14}N$ and $^{18}O/^{16}O$ in NO_3^-. The mean sampling resolution for these measurements was ca. 1.8 a^{-1} (i.e., ca. 0.6 year per sample).

Another 8.7 m long firn core (AF-11) was drilled from the Austfonna ice cap on Nordaustlandet (Fig. 1, Table 1) in May 2011. The ice core was drilled from the bottom of a snow pit 1.73 m in depth. A PICO drill with an internal diameter of 7.8 cm was used. The core handling, transport

Table 1 Details of the snow and firn sampling sites across Svalbard.

Name	Site/collection date	Location/elevation a.s.l. (m)	Depth(m)	Depth, water equivalent (m)	Winter accumulation rate, water equivalent (m a^{-1})[a]	Mean annual air temperature (°C)
HF-1	Holtedahlfonna 12/04/2011	79.14°N, 13.39°E/1127	1.66	0.66	0.66	−10.7[b]
HF-2	Holtedahlfonna 14/04/2011	79.14°N, 13.39°E/1130	1.60	0.61	0.61	
KV	Kongsvegen 23/04/2011	78.75°N, 13.33°E/673	1.73	0.75	0.75	No data
LF-11	Lomonosovfonna 04/04/2011	78.82°N, 17.43°E/1202	7.59	3.77	0.40	−12.0[c]
AF-11	Austfonna 05/05/2011	79.83°N, 23.97°E/757	10.09	5.88	0.69	−8.3[d]

[a]For the period 2010–11, estimated from snowpits or the top of firn cores. [b]From stake 4.5 at Holtedahlfonna, ca. 20 km south-east and 400 m lower than the HF-1 and HF-2 sites (J. Kohler, pers. comm.). [c]Pohjola et al. (2002). [d]Schuler et al. (2013). Temperature measurements at ca. 400 m a.s.l.

and sampling procedures were the same as for the LF-11 core.

Snow pits

Three snow pits, 1.60–1.73 m deep, were sampled in 2011 on the Holtedahlfonna (HF) ice cap and Kongsvegen glacier (KV), close to Ny-Ålesund in western Spitsbergen. Another snow pit (AF-11snow), 1.5 m deep, was sampled at the 2011 firn coring site on Austfonna (Fig. 1, Table 1). In addition, the top 1.5 m of the LF-11 firn core, hereafter denoted LF-11snow, was sampled to characterize snowpack properties at the Lomonosovfonna site (see preceding section).

The snow pits were sampled at 10-cm resolution in accordance with International Trans-Antarctic Scientific Expedition protocol (Twickler & Whitlow 1997) using 50-mL clean high-density polyethylene tubes. All sampling materials and tubes had been pre-cleaned using methanol and 18 MΩ water and double-sealed in polyethylene bags.

Chemical analyses

Concentrations of nine major ions (Na^+, NH_4^+, K^+, Ca^{2+}, Mg^{2+}, Cl^-, Br^-, NO_3^- and SO_4^{2-}) in snow and firn samples were determined using a ProfIC850 ion chromatograph (IC; Metrohm, Herisau, Switzerland) at Uppsala University, Sweden. Hereafter, brackets are used to denote ionic concentrations, e.g., [Na^+]. Samples and standards were handled under a class 100 clean air hood, using powder-free gloves. Standards were prepared before analysis and stored frozen at −20°C. Shortly prior to analysis, samples and standards were melted at room temperature (with vial lids closed). They were then placed in the IC auto-sampler (with lids removed) and covered with aluminium foil to avoid any dust contamination. A minimum of 5 mL H_2O per sample was required to measure cations and anions. Calibration curves ($R \geq 0.9998$) were constructed using 12 standards in the concentration range 1–1000 μg L^{-1}. Samples with ionic concentrations greater than the highest standard were diluted automatically using the Dosino module, which is part of the ProfIC850 IC system. Three sample blanks consisting of >18 MΩ water were analysed at the beginning and the end of every sample batch. Check samples consisting of melted bulk snow collected in Ny-Ålesund or Uppsala, Sweden, were analysed for every 10 samples to assess the reproducibility of measurements within a given batch. The reproducibility was within 5% for each ion. Detection limits were calculated as the average plus 1.68 times the standard deviation (σ) of six separate blanks ($c_{\mathrm{blank}} + 1.68 \times \sigma_{\mathrm{blank}}$) and were below 5 μg L^{-1} for each ion. In this paper, major ion concentrations in samples are reported as charge-equivalent concentrations in units of μmol L^{-1}. With the exception of NO_3^-, the non-sea salt (nss) fractions of each ion in snow and firn were estimated from the mean seawater composition, following:

$$[nssX] = [X]_{total} - \left(\frac{[X]}{[Na^+]}\right)_{seawater} \times [Na^+]_{total}, \quad (1)$$

where X stands for a major ion (Supplementary Table S1).

The $^{18}O/^{16}O$ ratios of water in melted firn core samples were analysed at the Institute of Geology at Tallinn Technical University, Estonia, using two methods: a L2120-i water isotope analyser (Picarro, Santa Clara, CA, USA), using cavity ringdown spectroscopy technology, with a high precision vaporizer A0211 for the LF-11 core; and a Delta V Advantage mass spectrometer (Thermo Fisher Scientific, Waltham, MA, USA) with a GasBench II system for the AF-11 core (Thermo Fisher Scientific). Results are reported using the $\delta^{18}O$ notation:

$$\delta^{18}O_{H_2O} = \frac{\left(^{18}O/^{16}O\right)_{sample} - \left(^{18}O/^{16}O\right)_{VSMOW}}{\left(^{18}O/^{16}O\right)_{VSMOW}}, \quad (2)$$

where VSMOW is the Vienna Standard Mean Ocean Water international standard. The measurements were calibrated against both VSMOW and the Vienna Standard Light Antarctic Precipitation standards, and the reproducibility for $\delta^{18}O_{H_2O}$ was estimated to be ±0.1‰ (1σ for four to six replicate measurements).

Stable isotope ratios of $^{15}N/^{14}N$ and $^{18}O/^{16}O$ in NO_3^- were determined by mass spectrometry at the University of East Anglia, UK, after conversion of NO_3^- to N_2O by the denitrifier method (Casciotti et al. 2002; Kaiser et al. 2007). The method requires at least 10 nmol of NO_3^- (20 nmol being optimum) in not more than 11 mL of H_2O sample. Samples with [NO_3^-] < 0.9 μmol L^{-1} were pre-concentrated using a freeze-drying procedure (lyophilization). All samples were then filtered through 0.2 μm Minisart PES syringe filters (Sartorius, Goettingen, Germany), collected in clean 50-mL plastic tubes and kept frozen until analysis.

The stable isotope composition of N in NO_3^- is expressed using the $\delta^{15}N$ notation:

$$\delta^{15}N_{NO_3^-} = \frac{\left(^{15}N/^{14}N\right)_{sample} - \left(^{15}N/^{14}N\right)_{Air}}{\left(^{15}N/^{14}N\right)_{Air}}, \quad (3)$$

Citation: *Polar Research* 2015, *34*, 23246, http://dx.doi.org/10.3402/polar.v34.23246

where $(^{15}N/^{14}N)_{Air}$ is the mean $^{15}N/^{14}N$ ratio of N_2 gas in air. The stable isotope composition of $^{18}O/^{16}O$ in NO_3^- is expressed as $\delta^{18}O_{NO_3^-}$ relative to VSMOW. The overall precision of the measurements, taking into account that samples were measured in different batches and days, was estimated to be $\pm 0.4‰$ and $\pm 1‰$ (1σ) for $\delta^{15}N_{NO_3^-}$ and $\delta^{18}O_{NO_3^-}$, respectively.

Laboratory tests showed that pre-concentrating NO_3^- in samples by a factor of 10 increased $\delta^{15}N_{NO_3^-}$ by ca. 0.33‰. However, the actual pre-concentration factors for low $[NO_3^-]$ samples were in fact much lower (2.5 for snow, 6.7 for firn), and the effect of lyophilization on $\delta^{15}N_{NO_3^-}$ is therefore considered negligible relative to the range of $\delta^{15}N_{NO_3^-}$ variations that was observed in Svalbard snow and firn samples (typically $\pm 3‰$ at each site; see below). Lyophilization was also found to have no detectable effect on $\delta^{18}O_{NO_3^-}$. The $\delta^{15}N_{NO_3^-}$ were not corrected for ^{17}O excess ($\Delta^{17}O$), which may cause values reported here to be 1–2‰ too high (Coplen et al. 2004). However, for a given $\delta^{18}O_{NO_3^-}$, $\Delta^{17}O$ is expected to vary by at most 6‰ (Morin et al. 2008), which would require a maximum $\delta^{15}N_{NO_3^-}$ correction of $-0.3‰$ in our samples. Such a correction is negligible compared to the observed seasonal $\delta^{15}N_{NO_3^-}$ variations in Svalbard snow and firn. Unfortunately, owing to the low final liquid volumes in pre-concentrated samples, duplication of the $\delta^{15}N_{NO_3^-}$ and $\delta^{18}O_{NO_3^-}$ determinations was not feasible.

Low $[NO_3^-]$ or sample volumes also limited the number of snow pit samples in which $\delta^{15}N_{NO_3^-}$ and $\delta^{18}O_{NO_3^-}$ could be determined. Gaps therefore exist in the snow pit sample sequences for these measurements. As a consequence, annual mean values estimated from snow pit samples could be biased by high $[NO_3^-]$ in single depositional events, particularly given the large temporal variations observed in the snow pit data (see below). This is not an issue for the firn core samples, as each represents integrated snow accumulation over several months.

Dating of the firn cores and snow pits

The LF-11 and AF-11 firn cores were dated by counting seasonal cycles in $\delta^{18}O_{H_2O}$ using the winter minima as an annual reference. In addition, specific features in major ion profiles in the LF-11 core were correlated with those in a separate, previously dated core from Lomonosovfonna (Vega et al. 2015). In this way, the LF-11 and AF-11 cores were estimated to span the temporal ranges 2004–2011 and 2000–2010, respectively.

To date the snow pits, three prominent peaks in $[Cl^-]$, observed in all pits, were correlated with (presumably synchronous) peaks found in the dated LF-11 core (assigned to years 2011.3, 2011.2 and 2011.1). Dating snow layers between these points was done by linear interpolation. The different snow pits were estimated to contain snow accumulated since the summer of 2010, in good agreement with inferences from the stratigraphy and density profiles in each pit.

Air mass back-trajectories

To quantify the relative influence of different aerosol source regions over Svalbard during the snow/firn sampling period 2010–11, we calculated trajectories of air masses arriving at Austfonna (Nordaustlandet) and Holtedahlfonna (Spitsbergen) during precipitation events, using the National Oceanic and Atmospheric Administration's Hybrid Single-Particle Lagrangian Integrated Trajectory model (HYSPLIT; Draxler & Hess 1998). Precipitation events were identified from hourly snow surface height measurements by sonic rangers (model SR50, Campbell Scientific, Logan, UT, USA) installed on automatic weather stations (AWS) at these sites. The first AWS is located on Etonbreen (370 m a.s.l.) on the western side of Austfonna (data provided by T.V. Schuler, University of Oslo; see Schuler et al. 2013). The second AWS is situated at 690 m a.s.l. on Holtedahlfonna (data provided by J. Kohler, NPI). Precipitation events detected at these AWS were assumed to have also occurred at the snow pit sites. The AWS snow height data were first smoothed using a 24 h running average. A snow event was defined as an increase in the smoothed surface snow height data series that exceeded 0.5 cm over a 6-h period.

Due to the variable duration of precipitation events, air mass back-trajectories were calculated at the start of each event over the period 12 August 2010 to 23 April 2011, which brackets the sampling period. Based on the estimated lifetime of NO_x in the Arctic (ca. 10 days; Liu et al. 1987), and the global mean lifetime of aerosol NO_3^- (four–six days; Xu & Penner 2012), we calculated air mass back-trajectories over five days, arriving 500 m above the Austfonna and Holtedahlfonna sampling sites. Such trajectories to Svalbard are expected to have lengths of 3000–5000 km (Eneroth et al. 2003), allowing for the identification of potential continental source regions of NO_x precursors to the measured NO_3^- in Svalbard snow and ice. Back-trajectories were computed using meteorological fields from the Global Data Assimilation System, and the clustering algorithm found in the HYSPLIT model was used to identify and map the most common trajectory types.

Results and discussion

Spatial variations in major ion concentrations

Mean concentrations of eight major ions measured in snow pits and firn core samples (Na^+, NH_4^+, K^+, Ca^{2+}, Mg^{2+}, Cl^-, Br^- and SO_4^{2-}) are given in Table 2. Nitrate is discussed separately. In a previous study, Semb et al. (1984) showed that the distribution of sea-salt ions (Cl^-, Na^+, SO_4^{2-} and Mg^{2+}) in snow across Svalbard is partly controlled by orographic effects, their concentrations decreasing with increased elevation and remoteness from the marine boundary layer. These authors also found that NO_3^-, NH_4^+ and non-sea salt sulphate ($nssSO_4^{2-}$) show decreasing concentrations from the south-east to the north-west sector of Svalbard. Similarly, we find that the concentrations of sea-salt ions in our snow pit samples are highest at the lower-elevation sites Kongsvegen (673 m a.s.l.) and Austfonna (757 m a.s.l.), presumably reflecting the dominance of marine aerosol sources in snow at these relatively low altitudes (Table 3). Our data also show that major ion concentrations in snow across Svalbard vary depending on the geographic situation relative to the orographic barrier formed by the mountains and uplands in north-central Spitsbergen (between ca. 14 and 17°E; Fig. 2). This is reflected in relatively higher ion concentrations in snow on Lomonosovfonna compared to Holtedahlfonna, despite similar elevations at these two sites (1202 and ca. 1130 m a.s.l). Indications of an east–west gradient in snow chemistry across Svalbard were reported by others for major ions (Beaudon et al. 2013), pesticides (Ruggirello et al. 2010) and BC (Forsström et al. 2009) in snow and firn.

Based on these observations, we chose to separate and group our sample data between eastern sites (Lomonosovfonna and Austfonna) and western sites (Holtedahlfonna and Kongsvegen) relative to longitude ca. 15°E. We then used the non-parametric Wilcoxon rank-sum test to compare the mean ion concentrations between the pooled data from the eastern and western sites (Gibbons & Chakraborti 2003). Only [$nssSO_4^{2-}$] and [$nssMg^{2+}$] displayed meaningful differences, their mean concentrations in snow at eastern Svalbard sites being significantly greater than at western sites ($\alpha = 0.1$). Remarkably high concentrations of [$nssCl^-$] and [$nssK^+$] were measured sporadically at Holtedahlfonna, Lomonosovfonna and Austfonna, and these outliers could mask some east–west differences in snow chemistry. Likewise, local terrestrial dust sources from snow-free terrain (e.g., nunataks) are known to supply $nssCa^{2+}$ and other ions in snowpacks of central Spitsbergen (Semb et al. 1984; Kang et al. 2001), and these local inputs could obscure larger-scale spatial variations in snow chemistry across the archipelago.

Spatial variations of $[NO_3^-]$, $\delta^{15}N_{NO_3^-}$ and $\delta^{18}O_{NO_3^-}$ in snow

The mean concentration and stable isotope composition ($\delta^{15}N_{NO_3^-}$ and $\delta^{18}O_{NO_3^-}$) of NO_3^- in Svalbard snow and firn samples are given in Table 4. Snow pit [NO_3^-] are similar at the three Spitsbergen sites (Holtedahlfonna, Lomonosovfonna and Kongsvegen), despite their different elevations. In contrast, snow samples from Austfonna (AF-11snow) have a mean [NO_3^-] that is twice that of the Spitsbergen sites. The $\delta^{15}N_{NO_3^-}$ and $\delta^{18}O_{NO_3^-}$ values

Table 2 Mean concentrations (charge equivalents; $\pm\sigma$) of major ions in seasonal snow at the sampling sites at Holtedahlfonna (HF), Kongsvegen (KV), Lomonosovfonna (LF) and Austfonna (AF), Svalbard. For [NO_3^-], see Table 4.

Site (elevation a.s.l. m)		Cl^-	Br^-	SO_4^{2-}	Na^+	K^+	NH_4^+	Ca^{2+}	Mg^{2+}	Period
		(μmol L^{-1})								
HF-1 (1127)	Mean	18	0.02	3	11	0.3	0.5	2	3	Mid-2010 to mid-2011
	σ	21	0.02	2	11	0.3	0.3	2	4	
HF-2 (1130)	Mean	13	0.01	2	10	0.2	0.3	2	3	
	σ	12	0.01	1	10	0.2	0.2	3	2	
KV (673)	Mean	61	0.1	8	14	1	0.4	4	13	
	σ	75	0.1	9	13	1	0.4	4	16	
LF-11snow (1202)	Mean	42	0.03	6	34	3	0.4	5	9	
	σ	70	0.02	8	58	1	0.5	8	13	
AF-11snow (757)	Mean	61	0.1	9	39	1	0.9	2	10	
	σ	117	0.1	14	83	2	0.9	3	23	
LF-11 (1202)	Mean	13	0.01	2	10	0.2	0.5	3	3	2004–2011
	σ	30	0.01	4	25	0.5	0.5	5	6	
AF-11 (757)	Mean	12	0.02	1	9	0.2	0.6	2	1	2000–2011
	σ	7	0.01	1	5	0.1	0.4	1	1	

Citation: *Polar Research* 2015, *34*, 23246, http://dx.doi.org/10.3402/polar.v34.23246

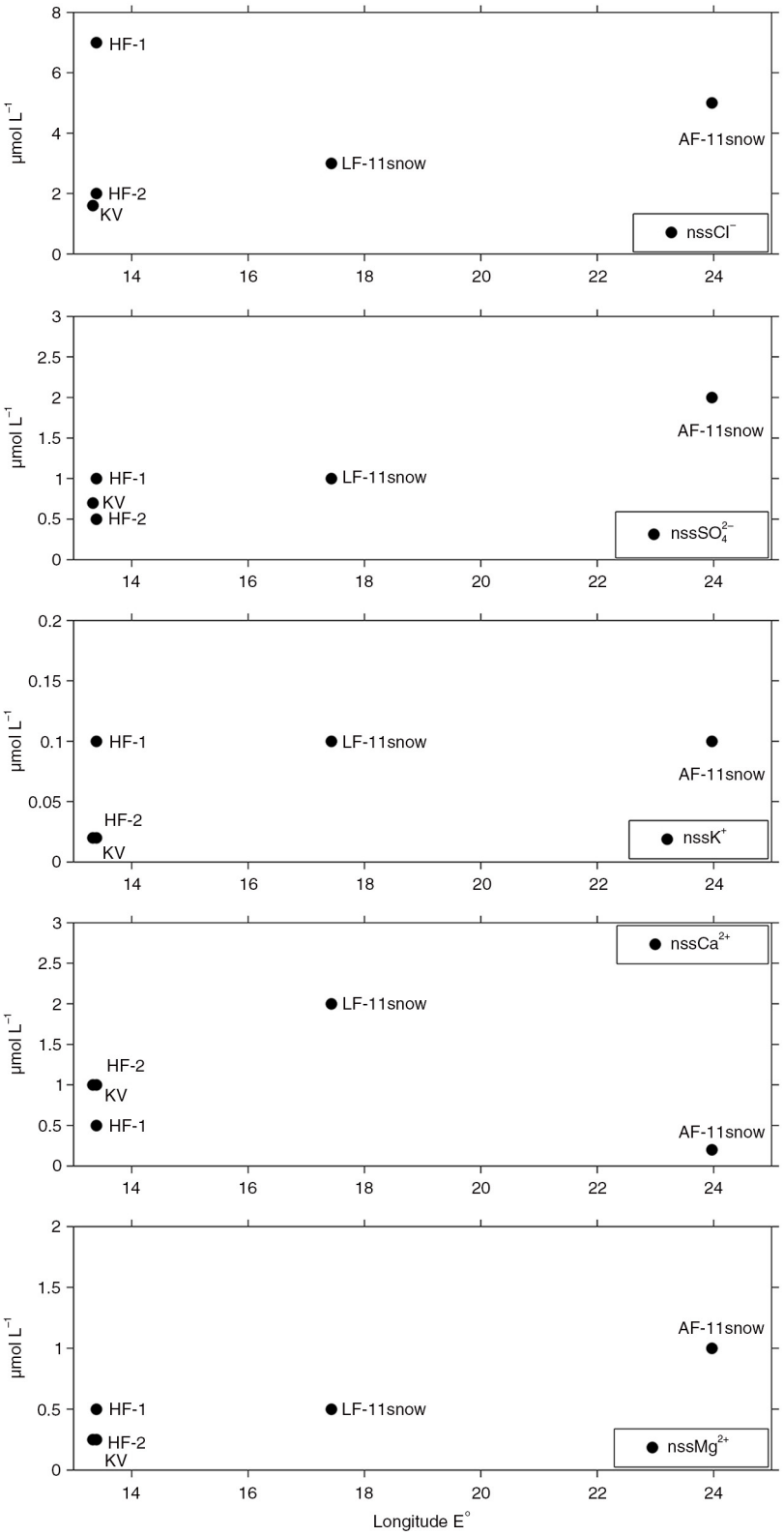

Fig. 2 West-to-east variations in mean non-sea salt (nss) ion concentrations measured in Svalbard snow pits and firn cores at Holtedahlfonna (HF), Kongsvegen (KV), Lomonosovfonna (LF) and Austfonna (AF).

Table 3 Non-sea salt (nss) ion concentration (charge equivalents; $\pm\sigma$) at the sampling sites at Holtedahlfonna (HF), Kongsvegen (KV), Lomonosovfonna (LF) and Austfonna (AF), Svalbard.

Site		$nssCl^-$	$nssSO_4^{2-}$	$nssK^+$	$nssCa^{2+}$	$nssMg^{2+}$	Period
		(μmol L^{-1})					
HF-1	Mean	7	2	0.1	1	1	
	σ	20	2	0.3	2	4	
HF-2	Mean	2	1.0	0.02	2	0.5	
	σ	1	0.5	0.02	3	0.4	
KV	Mean	1.6	1.4	0.02	2	0.5	mid-2010 to mid-2011
	σ	0.9	0.9	0.0.2	3	0.4	
LF-11snow	Mean	3	2	0.1	4	1	
	σ	3	2	0.1	7	2	
AF-11snow	Mean	5	4	0.1	0.4	2	
	σ	5	3	0.2	0.3	5	
LF-11	Mean	2	2	0.1	2	1	
	σ	3	2	0.2	4	1	2004–2011
AF-11	Mean	2	1	0.1	1	1	
	σ	1	1	0.1	1	1	2000–2011

show small local inter-site variations on Holtedahlfonna, but much larger variations at the regional scale, with higher $\delta^{15}N$ and lower $\delta^{18}O$ at the western Svalbard sampling sites (Fig. 3). Unlike for $[NO_3^-]$, these east–west differences were found to be statistically meaningful ($\alpha = 0.1$). A complementary analysis is provided in the supplementary material (Supplementary Section S1, Supplementary Table S2).

One factor that can affect spatial variations in $[NO_3^-]$ and its isotopic composition is the snow accumulation rate. In Svalbard, accumulation is highly variable due to the archipelago's complex topography and wind redistribution (Rasmussen & Kohler 2007). Figure 4 shows that for the winter 2010/11, winter snow accumulation across Svalbard (estimated from snow pits and firn cores) decreased almost linearly with increasing elevation ($R = 0.77$). However, neither $[NO_3^-]$ nor $\delta^{15}N_{NO_3^-}$ or $\delta^{18}O_{NO_3^-}$ shows any systematic, meaningful variations with snow accumulation or with elevation (Fig. 4, Supplementary Table S3).

Alternatively, the observed regional differences in $[NO_3^-]$, $\delta^{15}N_{NO_3^-}$ or $\delta^{18}O_{NO_3^-}$ in snow across Svalbard

Table 4 Mean values ($\pm\sigma$) of $\delta^{15}N_{NO_3^-}$, $\delta^{18}O_{NO_3^-}$ and $[NO_3]$ in seasonal snow at the sampling sites at Holtedahlfonna (HF), Kongsvegen (KV), Lomonosovfonna (LF) and Austfonna (AF), Svalbard.

Site		$\delta^{15}N_{NO_3^-}$ (‰)	$\delta^{18}O_{NO_3^-}$ (‰)	$[NO_3^-]$ (μmol L^{-1})	Period	$n^a([NO_3^-])$ n^a (δ)
HF-1	Average	−2	62	0.7	Mid-2010 to mid-2011	17
	σ	3	5	0.6		10
HF-2	Average	−1	59	0.7	Mid-2010 to mid-2011	18
	σ	3	3	0.4		13
KV	Average	−3	66	0.7	Mid-2010 to mid-2011	20
	σ	3	5	0.4		11
LF-11snow	Average	−11	80.99	0.7	Mid-2010 to mid-2011	24
	σ	1	0.03	0.5		2
AF-11snow	Average	Not measured		2	Mid-2010 to mid-2011	11
	σ			1		0
LF-11	Average	−9	76	1	2004–2011	156
	σ	3	4	1		12
AF-11	Average	−9	72	0.8	2000–2011	174
	σ	3	5	0.8		17

[a]Number of samples.

Citation: *Polar Research* 2015, *34*, 23246, http://dx.doi.org/10.3402/polar.v34.23246

could be explained by differences in the origin of air masses arriving at the eastern sites (Lomonosovfonna and Austfonna) and western sites (Holtedahlfonna and Kongsvegen). As mentioned before, air arriving at Svalbard may travel from both southerly and northerly directions (Hisdal 1998). Using air mass back-trajectory analyses over a decade, Eneroth et al. (2003) identified eight different air mass transport patterns to Ny-Ålesund in western Spitsbergen. Half of these originated in the Arctic Ocean, the others from northern Europe and/or Eurasia, or from the Atlantic sector. During spring and summer, low cyclonic activity and relatively stable weather conditions result in air masses being mostly confined to the Arctic Ocean. In contrast, during autumn and winter, more intense cyclonic activity results in enhanced transport of air masses from eastern North America, the North Atlantic and northern Europe/Eurasia. While there is low interannual variability in the relative frequency of these different air mass transport patterns, their seasonal or monthly frequency differs from year to year, mainly in response to variability in the strength of the Icelandic Low (Eneroth et al. 2003).

The air mass transport patterns described above may be adequate for interpreting snow and firn chemistry data from sites close to Ny-Ålesund, such as Holtedahlfonna or Lomonosovfonna. However, they may not be representative for sites further east on Nordaustlandet, such as Austfonna. In order to better discriminate the origin of air masses affecting our sampling sites, we analysed five-day back-trajectories associated with precipitation events at Holtedahlfonna ($N=54$) and Austfonna ($N=86$) during the snow pit sampling period (August 2010 to April 2011). At each of these sites, individual trajectories were clustered into three main transport patterns. Air masses arriving at Austfonna during precipitation events were mostly transported from the east (43%), west (36%) or south-west (21%), and westerly trajectories often originated from continental Eurasia (Figs. 5, 6). In contrast, most air masses arriving at Holtedahlfonna during precipitation events were mostly transported from the west (44%), north-east (31%) and south-west (24%), many of the latter trajectories passing over northern Europe (Figs. 7, 8).

The relative length of different air mass trajectories can affect the $\delta^{15}N$ of NO_3^- deposited in snow by limiting the time during which in-transport isotopic fractionation can occur (Freyer 1991). During airborne transport, NO_x undergoes oxidation reactions that produce NO_3^-. Isotopic fractionation of N accompanies some of these reactions, resulting in reactants and products with different $\delta^{15}N$. For any such reaction, the isotopic fractionation ε between product and reactant is defined as:

$$\varepsilon = (\delta^{15}N_{product} - \delta^{15}N_{reactant})/(1 + \delta^{15}N_{reactant}) \quad (4)$$

The reaction

$$^{15}NO + {}^{14}NO_2 \rightleftharpoons {}^{14}NO + {}^{15}NO_2 \quad (5)$$

is often accompanied by equilibrium isotopic fractionation with $\varepsilon > 0$, where the more oxidized compound is considered to be the product. In contrast, the reaction

$$NO_2 + OH \xrightarrow{M} HNO_3 \quad (6)$$

is accompanied by kinetic fractionation with $\varepsilon < 0$ because the ^{14}N isotopologue reacts faster than the ^{15}N isotopologue, lowering the $\delta^{15}N$ of the products relative to the reactants (Heaton 1987 and references therein).

Vega et al. (2015) estimated the magnitude of in-transport fractionation effects on $\delta^{15}N_{NO_3^-}$ using a simple isotopic mass balance model (Freyer et al. 1996) applied to $\delta^{15}N_{NO_3^-}$ data from pre-industrial (pre-1900) and modern (post-1950) ice-core samples obtained from Lomonosovfonna in eastern Spitsbergen. The anthropogenic contribution ($\delta^{15}N_{ant}$) to the $\delta^{15}N$ of ice-core NO_3^- was calculated as:

$$\delta^{15}N_{ant} = f_{comb}\delta^{15}N_{comb} + (1 - f_{comb})\delta^{15}N_{soil}, \quad (7)$$

where $\delta^{15}N_{comb}$, $\delta^{15}N_{soil}$ are the estimated mean isotopic compositions of NO_x from anthropogenic fossil fuel combustion ($-13‰ \le \delta^{15}N \le 20‰$; Hastings 2010; Felix et al. 2012) and from soil emissions ($-48.9 \le \delta^{15}N \le -19.9‰$; Li & Wang 2008), respectively. The variables f_{comb} and f_{soil} are estimated NO_x emission fractions from the most likely source regions to Svalbard, the latter being, over the period between 1970 and 2008, the USA, the European countries belonging to the Organisation for Economic Co-operation and Development and the Russian Federation (Samyn et al. 2012). Plausible values for f_{comb} and f_{soil} were obtained from the European Commission's Emission Database for Global Atmospheric Research (EC-JRC/PBL 2011; Supplementary Table S4).

Using these data, the magnitude of in-transport fractionation effects (ε_{trans}) on $\delta^{15}N$ of ice-core NO_3^- could be estimated by:

$$\varepsilon_{trans} = \frac{\left[\frac{\delta^{15}N_{post-1950} - f\delta^{15}N_{pre-1900}}{1-f}\right] - \delta^{15}N_{ant}}{1+\delta^{15}N_{ant}}, \quad (8)$$

where f is the ratio of the mean $[NO_3^-]$ in pre-1900 ice (0.6 μmol L^{-1}) and the mean $[NO_3^-]$ in the whole core

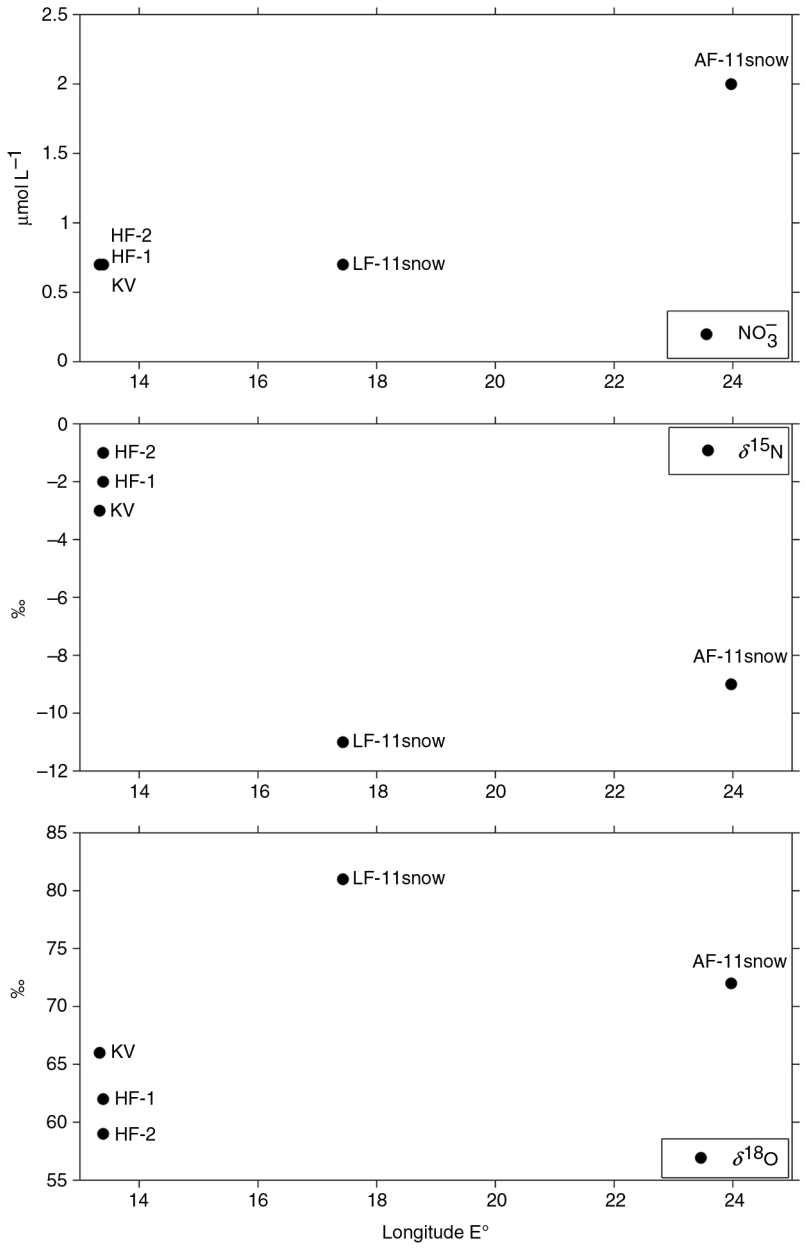

Fig. 3 West-to-east variations in the mean $[NO_3^-]$, $\delta^{15}N_{NO_3^-}$ and $\delta^{18}O_{NO_3^-}$ determined in Svalbard snow pits and firn cores at Holtedahlfonna (HF), Kongsvegen (KV), Lomonosovfonna (LF) and Austfonna (AF). For AF-11, the $\delta^{15}N_{NO_3^-}$ and $\delta^{18}O_{NO_3^-}$ values shown were determined from firn core samples as values in seasonal snow could not be obtained.

(0.9 µmol L^{-1}). Results suggest that on Lomonosovfonna, the contribution of (non-source related) in-transport fractionation effects (ε_{trans}) to the $\delta^{15}N_{NO_3^-}$ in snow could be as large as ca. −32‰. A similar calculation has not yet been performed for other Svalbard sites owing to the limited $\delta^{15}N_{NO_3^-}$ data available. However, the estimated ε_{trans} from Lomonosovfonna underscores how source-related signatures in $\delta^{15}N_{NO_3^-}$ could be obscured by in-transport fractionation as a function of air mass transport distance.

Evidence for such in-transport fractionation effects may be found in measurements of $\delta^{15}N_{NO_3^-}$ in snowfall at Ny-Ålesund reported by Heaton et al. (2004). A precipitation event on 23 April 2001 delivered snow with a $[NO_3^-]$ of 2 µmol L^{-1} and a $\delta^{15}N_{NO_3^-}$ of −17‰, while a later event on 5 April 2002 delivered snow with a $[NO_3^-]$ of 4 µmol L^{-1}

Citation: *Polar Research* 2015, *34*, 23246, http://dx.doi.org/10.3402/polar.v34.23246

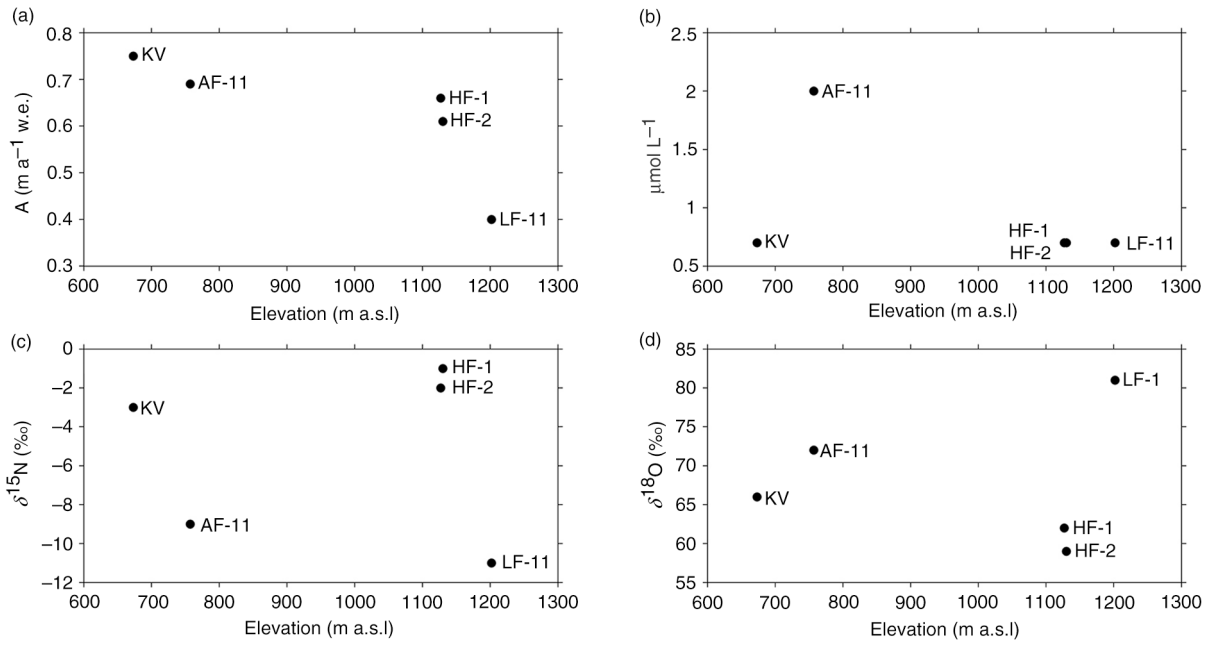

Fig. 4 Altitudinal variations in (a) the estimated snow accumulation rate for winter 2010/11; and mean values of (b) $[NO_3^-]$ (µmol L^{-1}), (c) $\delta^{15}N_{NO_3^-}$ (‰) and (d) $\delta^{18}O_{NO_3^-}$ (‰) in snow and firn at Holtedahlfonna (HF), Kongsvegen (KV), Lomonosovfonna (LF) and Austfonna (AF).

and a $\delta^{15}N_{NO_3^-}$ of −9‰. An analysis of associated air mass back-trajectories for the two snowfall events (Fig. 9) shows that their contrasting $[NO_3^-]$ and $\delta^{15}N_{NO_3^-}$ values could be explained by different air mass sources and transport routes. The air mass trajectory for the snowfall on 23 April 2001 passed over Alaska and the Arctic Ocean (Fig. 9a), while the trajectory for the snowfall on 5 April 2002 passed over the North Atlantic, close to England and

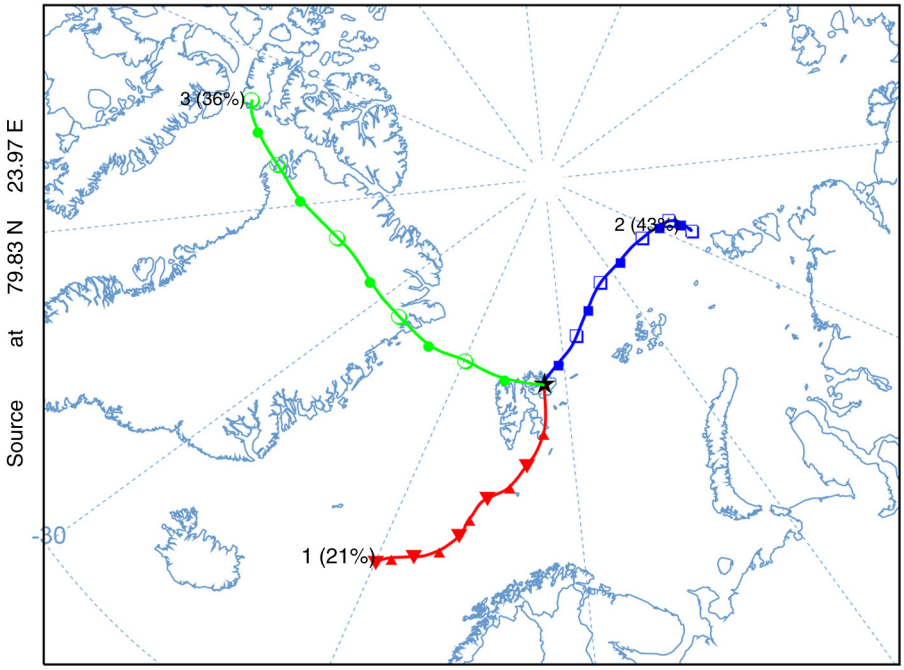

Fig. 5 Clustered mean five-day back-trajectories of air masses arriving at Austfonna, Nordaustlandet, calculated for 86 precipitation events recorded between 12 August 2010 and 23 April 2011. Data from the Global Data Assimilation System (GDAS).

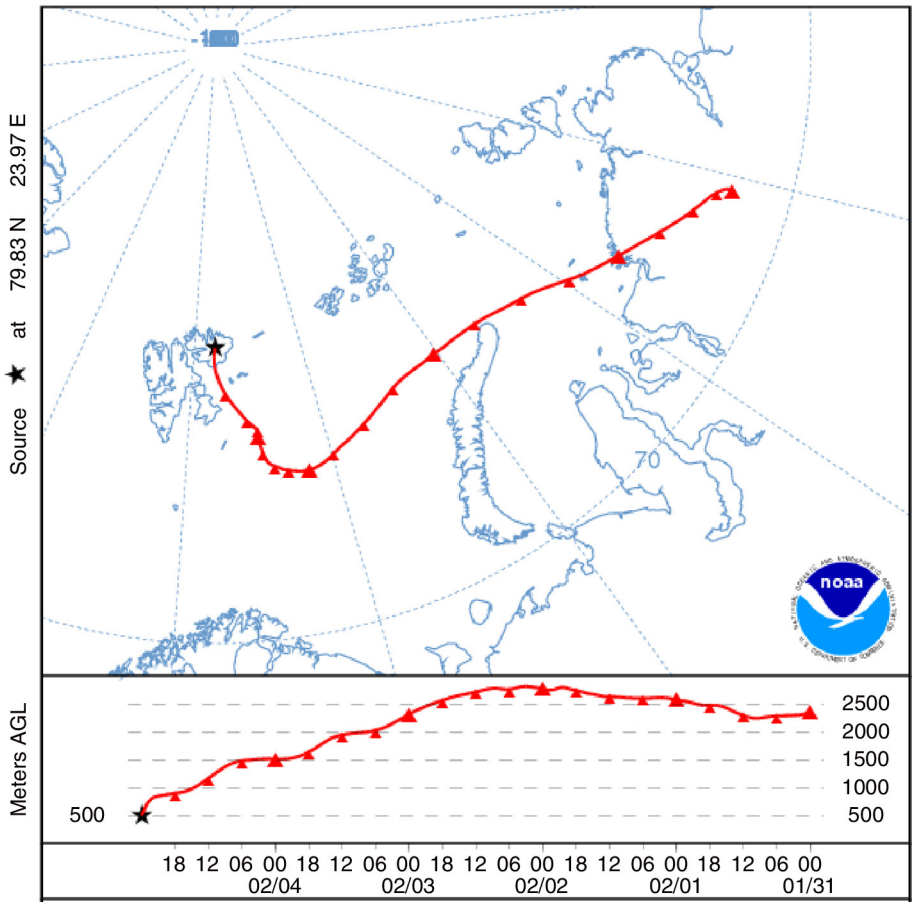

Fig. 6 Five-day back-trajectory for a precipitating air mass arriving at Austfonna, Nordaustlandet, on 6 February 2011. Data from the Global Data Assimilation System (GDAS) using the National Oceanic and Atmospheric Administration's Hybrid Single-Particle Lagrangian Integrated Trajectory model (HYSPLIT).

Scandinavia, and this air mass is therefore more likely to have mixed with polluted air from these regions (Fig. 9b). However the most fractionated value of $\delta^{15}N_{NO_3^-}$ was that associated with the 23 April 2001 snowfall, which had the lowest $[NO_3^-]$. This suggests that snow delivered by air masses that travel long distances over the Arctic Ocean may inherit lower $\delta^{15}N_{NO_3^-}$ owing to extensive in-transport fractionation, when compared with snow delivered by (often polluted) air masses arriving more directly to Svalbard from northern Europe/Eurasia.

We therefore speculate that glacier sites in Svalbard that receive snowfall predominantly associated with relatively short/fast air mass trajectories from northern Europe/Eurasia are more likely to preserve $\delta^{15}N_{NO_3^-}$ signatures from NO_x source emissions, anthropogenic or otherwise. This should be the case on Holtedahlfonna or Kongsvegen, for example. Verification of this hypothesis will require an estimation of ε_{trans} using measurements of $\delta^{15}N_{NO_3^-}$ in pre-industrial ice-core samples (as described above), which are presently unavailable.

Seasonal variability of $[NO_3^-]$, $\delta^{15}N_{NO_3^-}$ and $\delta^{15}N_{NO_3^-}$ in snow

Temporal variations of $[NO_3^-]$, $\delta^{15}N_{NO_3^-}$ and $\delta^{18}O_{NO_3^-}$ in snow over the period 2010–11, reconstructed from snow pits on Holtedahlfonna and Kongsvegen (western Svalbard sites), are presented on Fig. 10. Also shown are $[NO_3^-]$, and $\delta^{15}N_{NO_3^-}$ measured in fresh snow at Ny-Ålesund in spring 2001 and 2002 (Heaton et al. 2004). Decadal-scale variations in $[NO_3^-]$, $\delta^{15}N_{NO_3^-}$ and $\delta^{18}O_{NO_3^-}$ reconstructed from firn cores are discussed separately in the following section.

In many, but not all, snow pits, higher $[NO_3^-]$ (up to 3 μmol L^{-1}) are found in snow layers deposited in autumn and/or winter compared to spring. Exceptions are Austfonna (AF-11snow), where the highest $[NO_3^-]$ is in spring snow, and Lomonosovfonna (LF-11snow), where $[NO_3^-]$ is highest in summer snow layers. For comparison, at Barrow, Alaska, and at Alert, Canada, atmospheric $[NO_3^-]$ reach a seasonal maximum during

Citation: *Polar Research* 2015, *34*, 23246, http://dx.doi.org/10.3402/polar.v34.23246

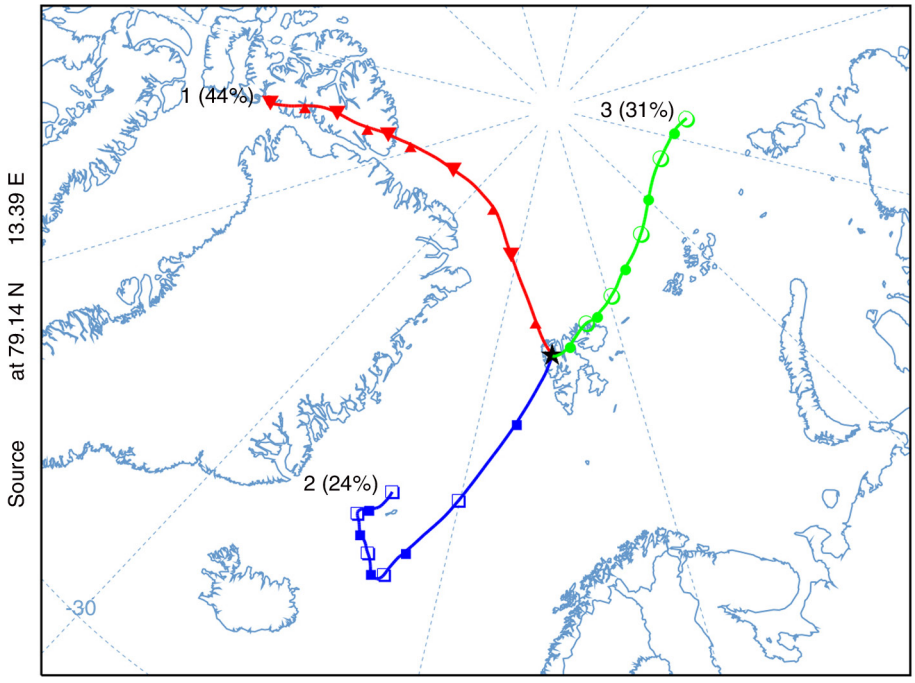

Fig. 7 Clustered mean five-day back-trajectories of air masses arriving at Holtedahlfonna, Spitsbergen, calculated for 54 precipitation events recorded between 12 August 2010 and 23 April 2011. Data from the Global Data Assimilation System (GDAS).

the period March–April, coincident with the highest incidence of Arctic Haze events at this sites (Morin et al. 2007; Quinn et al. 2007; Morin et al. 2012; see also the Supplementary file). In contrast, [NO_3^-] in central Greenland snow tends to peak during spring and summer rather than in autumn and winter, although seasonal variations are not always easy to resolve (Burkhart et al. 2004; Hastings et al. 2004). Reported higher [NO_3^-] in central Greenland have been attributed to the greater influence of polluted air masses transported from North America during this season (Kahl et al. 1997).

Figure 10b and c present seasonally-averaged $\delta^{15}N_{NO_3^-}$ and $\delta^{18}O_{NO_3^-}$ in the different snow pits sampled across Svalbard. The $\delta^{15}N_{NO_3^-}$ measured in fresh snow at Ny-Ålesund by Heaton et al. (2004) are also shown, but not their $\delta^{18}O_{NO_3^-}$ because the analytical method they employed differed from the one used in this work. The observed range of $\delta^{15}N_{NO_3^-}$ and $\delta^{18}O_{NO_3^-}$ values in Svalbard snow is narrower than that observed at Summit, Greenland (Hastings et al. 2004), but the difference could be explained by the limited number of summer snow samples in our data.

The snow pits share some features, the lowest $\delta^{15}N_{NO_3^-}$ being apparently associated with winter or spring snow layers (Fig. 10b). In central Greenland, Hastings et al. (2004) reported higher $\delta^{15}N_{NO_3^-}$ in spring/summer snow relative to autumn/winter snow. They attributed these variations to seasonal changes in the dominant source contributions of NO_3^-: higher spring/summer $\delta^{15}N_{NO_3^-}$ were ascribed to greater biomass burning, biogenic soil emissions and lightning NO_x emissions in these seasons, compared to greater fossil fuel combustion emissions in autumn/winter. Our snow pit data from Svalbard, although limited, appear to show a similar seasonal pattern, and the source-related interpretation proposed by Hastings et al. (2004) for Greenland probably holds true for these sites also (Fig. 10). In Svalbard, higher $\delta^{15}N_{NO_3^-}$ in summer snow could be associated in part with NO_x emissions from forest fires in Siberia (Stohl et al. 2007).

Local post-depositional effects, such as evaporation or photolysis, could also contribute to the relatively high $\delta^{15}N_{NO_3^-}$ observed in spring snow layers at one of the Holtedahlfonna sites (HF-2). However, based on findings by Beine et al. (2003), Amoroso et al. (2006) and Björkman (2013), we do not expect photolysis to be a major factor of $\delta^{15}N_{NO_3^-}$ variability in snow at this site. Other, non-source-related processes that can lead to increased $\delta^{15}N_{NO_3^-}$ in springtime snow are desorption of HNO_3 (Honrath et al. 1999; Dibb et al. 2002; Röthlisberger et al. 2002; Blunier et al. 2005) or wind action that mixes surficial snow layers, thereby altering the $\delta^{15}N_{NO_3^-}$ in the affected snow strata. However, our data are too limited to allow us these effects to be quantified.

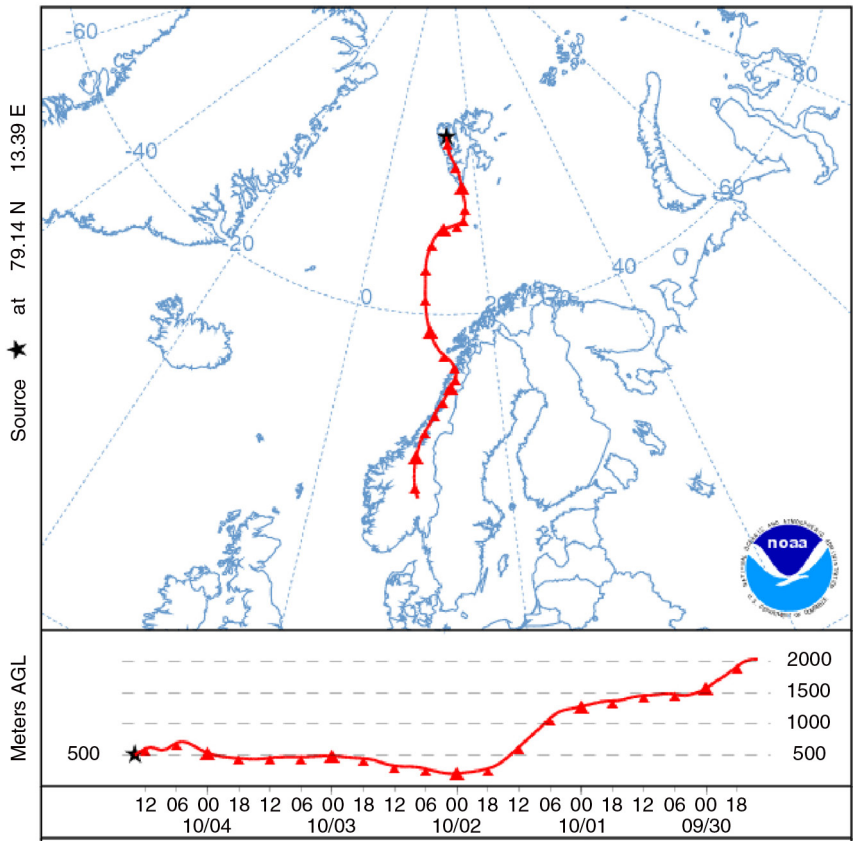

Fig. 8 Five-day back-trajectory for a precipitating air mass arriving at Holtedahlfonna, Spitsbergen, on 4 October 2010. Data from the Global Data Assimilation System (GDAS) using the National Oceanic and Atmospheric Administration's Hybrid Single-Particle Lagrangian Integrated Trajectory model (HYSPLIT).

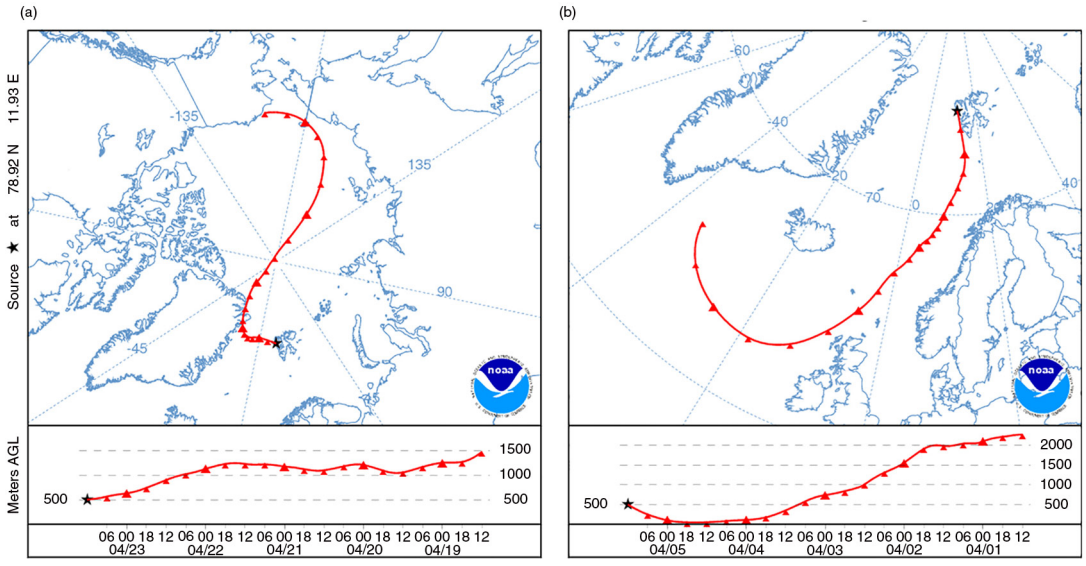

Fig. 9 Five-day air mass back-trajectories for the snowfall events reported by Heaton et al. (2004) at Ny-Ålesund during (a) 2001 and (b) 2002. Data from the Climate Diagnostics Center (CDC) using the National Oceanic and Atmospheric Administration's Hybrid Single-Particle Lagrangian Integrated Trajectory model (HYSPLIT).

Citation: *Polar Research* 2015, *34*, 23246, http://dx.doi.org/10.3402/polar.v34.23246

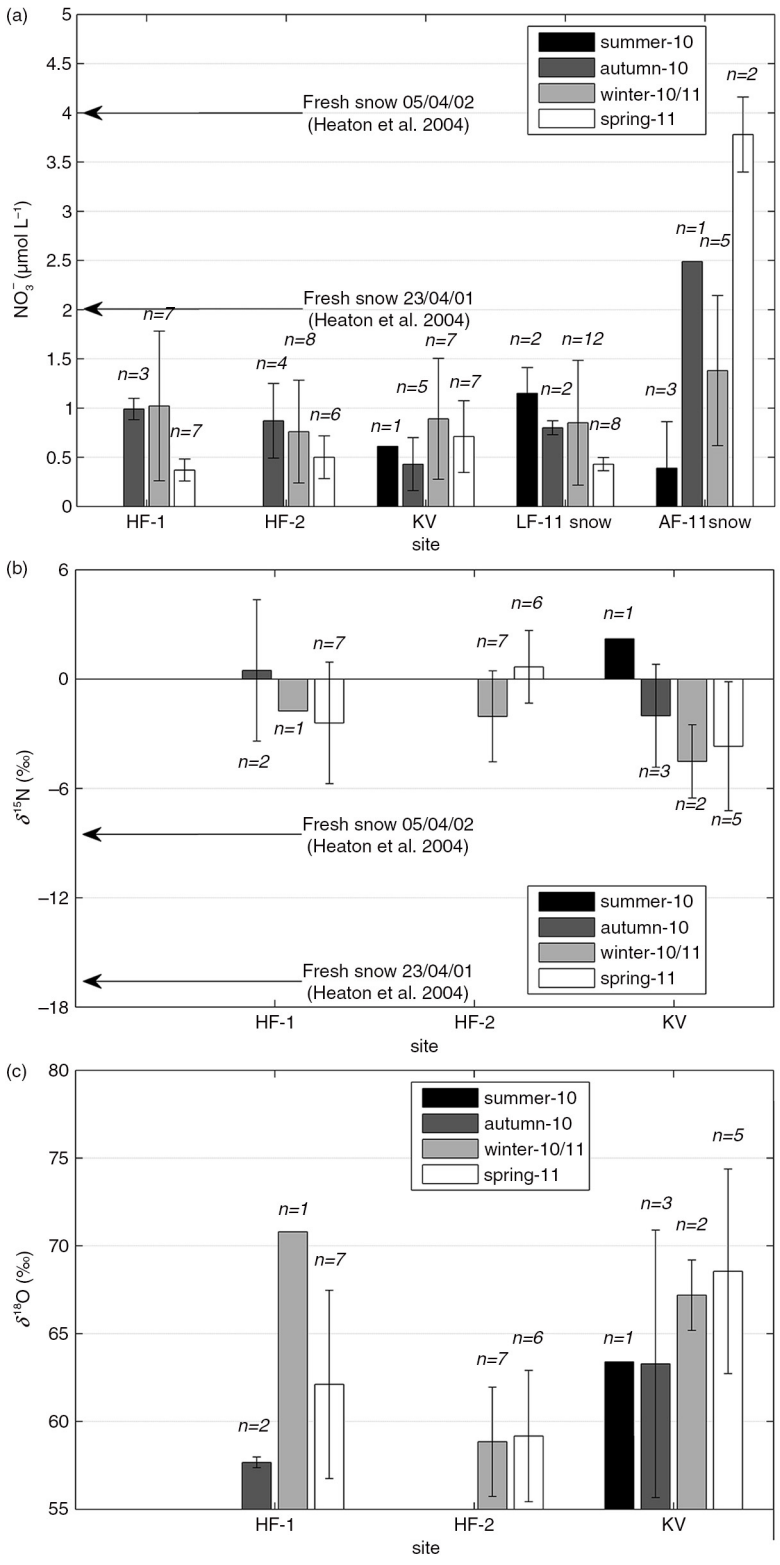

Fig. 10 Comparison of estimated seasonal mean values ($\pm 1\sigma$) of (a) [NO_3^-], (b) $\delta^{15}N_{NO_3^-}$ and (c) $\delta^{18}O_{NO_3^-}$ in snowpits at sampling sites across Svalbard: Holtedahlfonna (HF), Kongsvegen (KV), Lomonosovfonna (LF) and Austfonna (AF). The [NO_3^-] measured in snowfall at Ny-Ålesund in 2001 and 2002 and reported by Heaton et al. (2004) is marked with horizontal arrows.

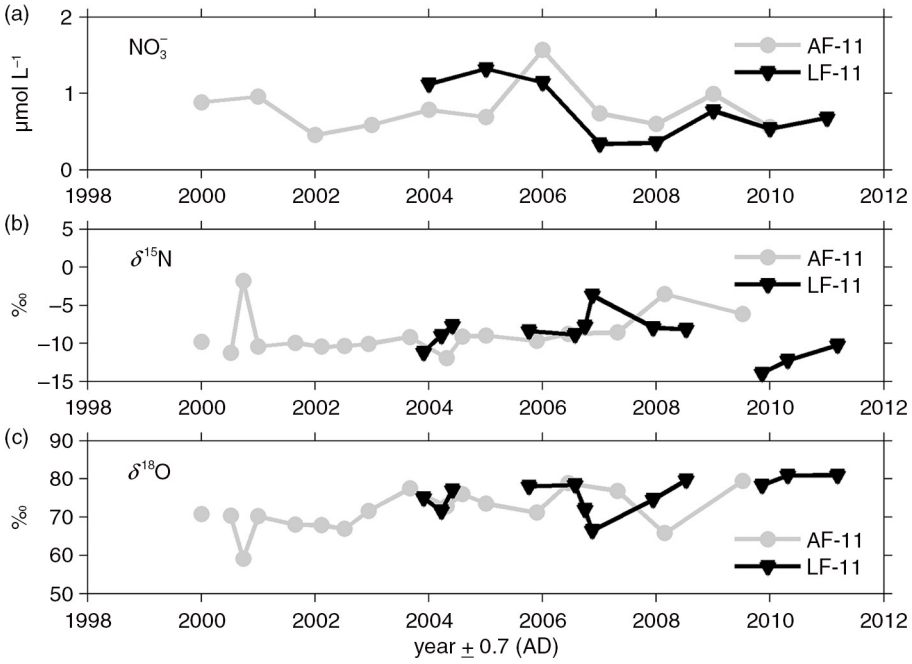

Fig. 11 (a) Annual mean values of (a) $[NO_3^-]$, (b) $\delta^{15}N_{NO_3^-}$ and (c) $\delta^{18}O_{NO_3^-}$ measured in the AF-11 and LF-11 firn cores from Austfonna and Lomonosovfonna, respectively. The resolution of the isotopic measurements in the cores is 1.8 samples a^{-1}. The mean error in the dating of the cores was estimated as ±0.7 a.

The $\delta^{18}O_{NO_3^-}$ in Svalbard snow pits range between 50 and 80‰ (Fig. 10c), the lower value being ca. 10‰ lower than reported values for Greenland snow (Hastings et al. 2004). The data do not show a very clear seasonality. However, where such a comparison is possible, $\delta^{18}O_{NO_3^-}$ values are relatively higher in winter/spring snow layers compared to summer/autumn layers, possibly as a result of seasonal changes in the dominant oxidation pathways leading to the formation of NO_3^- (e.g., Michalski et al. 2003; Morin et al. 2008).

Decadal variability of $[NO_3^-]$, $\delta^{15}N_{NO_3^-}$ and $\delta^{18}O_{NO_3^-}$ in firn cores

Variations of $[NO_3^-]$, $\delta^{15}N_{NO_3^-}$ and $\delta^{18}O_{NO_3^-}$ in firn over the period 2000–2011, as reconstructed from the AF-11 (Austfonna) and LF-11 (Lomonosovfonna) cores, are presented on Fig. 11. Despite differences between coring site locations and elevations (Table 1), the mean $[NO_3^-]$ in the two cores is comparable: 0.8±0.8 µmol L^{-1} in AF-11, and 1.0±1.0 µmol L^{-1} in LF-11 (Table 4). The $\delta^{15}N_{NO_3^-}$ and $\delta^{18}O_{NO_3^-}$ were measured at a lower resolution in firn cores (mean ca. 1.8 samples a^{-1}) than in snow pits (10 samples a^{-1}). Therefore, the $\delta^{15}N_{NO_3^-}$ and $\delta^{18}O_{NO_3^-}$ in the firn core samples should represent the composite, integrated signatures of different NO_3^- transport and deposition episodes over one or 2 years. From observations on a glacier near Ny-Ålesund, Björkman et al. (2013) estimated that dry deposition accounted for only ca. 14% (average) of total NO_3^- deposition in snow at that site between 2009 and 2010. Considering also that over recent decades most precipitation in Svalbard occurred in autumn and winter (Førland et al. 2011), we expect that $[NO_3^-]$, $\delta^{15}N_{NO_3^-}$ and $\delta^{18}O_{NO_3^-}$ in the LF-11 and AF-11 firn cores are likely to be biased towards winter values. The mean $\delta^{15}N_{NO_3^-}$ and $\delta^{18}O_{NO_3^-}$ are closely comparable in the two firn cores: $\delta^{15}N = -9 \pm 3‰$ in both AF-11 and LF-11; $\delta^{18}O = 72 \pm 5‰$ and 76±4‰ in AF-11 and LF-11, respectively. These results indicate that the combined isotopic imprint of NO_x sources, in-transport and/or post-depositional processes that define the $\delta^{15}N_{NO_3^-}$ and $\delta^{18}O_{NO_3^-}$ in snow were similar at the two eastern Svalbard sites over the past decade.

Conclusions

Analyses of seasonal snow and firn samples collected in 2010–11 at four glacier sites across the Svalbard Archipelago did not reveal significant spatial variations in major ion concentrations, save for $[nssSO_4^{2-}]$ and $[nssMg^{2+}]$, which were higher in accumulated snow at sites on eastern Spitsbergen and Nordauslandet (eastern sites) compared to sites located on western Spitsbergen (western sites). Results also show the existence of zonal

Citation: *Polar Research* 2015, *34*, 23246, http://dx.doi.org/10.3402/polar.v34.23246

differences in the isotopic composition of NO_3^- in snow across the archipelago, with lower nitrate $\delta^{15}N_{NO_3^-}$ and higher $\delta^{18}O_{NO_3^-}$ measured at eastern sites compared to western sites. Air mass back-trajectories suggest that these contrasts are due to differences in the sources region(s) and/or transport pathway(s) of precipitating air masses, transport from the Arctic Ocean and northern Eurasia being relatively more frequent at Austfonna (Nordaustlandet), and transport from northern Greenland and the Canadian High Arctic more frequent on north-western Spitsbergen (Holtedahlfonna). The frequency of fast and direct air mass transport from the north-west Atlantic sector and from northern Europe may also be slightly greater over the western sector of Svalbard. We suggest that snow deposited during precipitation episodes associated with long-distance air mass transport over the Arctic Ocean tend to inherit relatively low $\delta^{15}N_{NO_3^-}$ due to in-transport N isotope fractionation processes. In contrast, faster air mass transport from the south–south-west (north-west Atlantic, northern Europe) to Svalbard may result in snowfall with relatively higher $\delta^{15}N_{NO_3^-}$ because in-transport fractionation of N is then more time-limited. If the western sector of Svalbard is, as we suspect, more frequently exposed to such southerly air mass incursions, the snowpacks in this region may therefore better preserve the $\delta^{15}N_{NO_3^-}$ fingerprint of anthropogenic NO_x sources from western Europe. Future additional sampling and analysis of snowpacks and firn from this sector of Svalbard would allow verification of these inferences.

The findings presented in this paper improve our the understanding of the different sources, source regions and factors affecting atmospheric N_r deposition over the Svalbard Archipelago, and also provide useful information to constrain the interpretation of ice-core records of temporal NO_3^- deposition trends in this sector of the Arctic.

Acknowledgements

The authors thank the ice-coring teams and NPI for field logistical support. J. Kohler (NPI) and T.V. Schuler (University of Oslo) kindly provided the AWS data. This study was supported within the Marie Curie Initial Training Network NSINK ITN-2007.1.1, ENV. 215503, with additional support from NPI, Stiftelsen Ymer-80 and the Geographical Society of Uppsala, Sweden. This is a contribution to the Cryosphere–Atmosphere Interactions in a Changing Arctic Climate Top-level Research Initiative and to the EU Regional Development Foundation, project 3.2.0801.12-0044. Insightful comments by two anonymous referees improved the manuscript. At the time of this research, MPB was working at the Norwegian Polar Institute, Fram Centre, P.O. Box 6606 Langnes, NO-9296 Tromsø, Norway.

References

Aanes R., Sæther B.-E. & Øritsland N.A. 2000. Fluctuations of an introduced population of Svalbard reindeer: the effects of density dependence and climatic variation. *Ecography 23*, 437–443.

Amoroso A., Beine H.J., Sparapani R., Nardino M. & Allegrini I. 2006. Observation of coinciding Arctic boundary layer ozone depletion and snow surface emissions of nitrous acid. *Atmospheric Environment 40*, 1949–1956.

Atkin O.K. 1996. Reassessing the nitrogen relations of Arctic plants: a mini-review. *Plant Cell Environment 19*, 695–704.

Beaudon E., Moore J.C., Martma T., Pohjola V.A., van de Wal R.S.W., Kohler J. & Isaksson E. 2013. Lomonosovfonna and Holtedahlfonna ice cores reveal east–west disparities of the Spitsbergen environment since AD 1700. *Journal of Glaciology 59*, 1069–1083.

Beine H.J., Dominé F., Ianniello A., Nardino M., Allegrini I., Teinilä K. & Hillamo R. 2003. Fluxes of nitrates between snow surfaces and the atmosphere in the European High Arctic. *Atmospheric Chemistry and Physics 3*, 335–346.

Björkman M.P. 2013. *Nitrate dynamics in the Arctic winter snowpack*. Faculty of Mathematics and Natural Sciences, University of Oslo, Dissertation Series 1397. Oslo: Akademika Publishing.

Björkman M.P., Kühnel R., Patridge D.G., Roberts T.J., Aas W., Mazzola M., Viola A., Hodson A., Ström J. & Isaksson E. 2013. Nitrate dry deposition in Svalbard. *Tellus B 65*, article no. 19071, doi: 10.3402/tellusb.v65i0.19071.

Björkman M.P., Zarsky J.D., Kühnel R., Hodson A., Settler B. & Psenner R. 2014. Microbial cell retention in a melting High Arctic snowpack, Svalbard. *Arctic, Antarctic and Alpine Research 46*, 471–482.

Blunier T., Floch G.L., Jacobi H.-W. & Quansah E. 2005. Isotopic view on nitrate loss in Antarctic surface snow. *Geophysical Research Letters 32*, L13501, doi: 10.1029/2005GL023011.

Bottenheim J.W., Gallant A.G. & Brice K.A. 1986. Measurements of NO_y species and O_3 at 82°N latitude. *Geophysical Research Letters 13*, 113–116.

Brimblecombe P., Tranter M., Abrahams P.W., Blackwood I., Davies T.D. & Vincent C.E. 1985. Relocation and preferential elution of acidic solute through the snowpack of a small, remote, high-altitude Scottish catchment. *Annals of Glaciology 7*, 141–147.

Burkhart J.F., Hutterli M., Bales R.C. & McConnell J.R. 2004. Seasonal accumulation timing and preservation of nitrate in firn at Summit, Greenland. *Journal of Geophysical Research—Atmospheres 109*, D19302, doi: 10.1029/2004JD004658.

Carroll M.A. & Thompson A.M. 1995. NO_x in the non-urban troposphere. In J.R. Barker (ed.): *Progress and problems*

in atmospheric chemistry. Pp. 198–255. Singapore: World Scientific.

Casciotti K.L., Sigman D.M., Hastings M.G., Böhlke J.K. & Hilkert A. 2002. Measurement of the oxygen isotopic composition of nitrate in seawater and freshwater using the denitrifier method. *Analytical Chemistry 74*, 4905–4912.

Coplen T.B., Böhlke J.K. & Casciotti K.L. 2004. Using dual-bacterial denitrification to improve $\delta^{15}N$ determinations of nitrates containing mass-independent ^{17}O. *Rapid Communications in Mass Spectrometry 18*, 245–250.

Dibb J.E., Arsenault M., Peterson M.C. & Honrath R.E. 2002. Fast nitrogen oxide photochemistry in Summit, Greenland snow. *Atmospheric Environment 36*, 2501–2511.

Dickson L.G. 2000. INSTAAR constraints to nitrogen fixation by cryptogamic crusts in a polar desert ecosystem, Devon Island, N.W.T., Canada. *Arctic, Antarctic, and Alpine Research 32*, 40–45.

Draxler R.R. & Hess G.D. 1998. An overview of the HYSPLIT_4 modeling system of trajectories, dispersion, and deposition. *Austrian Meteorological Magazine 47*, 295–308.

EC-JRC/PBL (European Commission, Joint Research Centre/ Netherlands Environmental Assessment Agency). 2011. Emissions Database for Global Atmospheric Research (EDGAR) version 4.2. Accessed on the internet at http://edgar.jrc.ec.europa.eu on 12 August 2013.

Eneroth K., Kjellström E. & Holmén K. 2003. A trajectory climatology for Svalbard; investigating how atmospheric flow patterns influence observed tracer concentrations. *Physics and Chemistry of the Earth 28*, 1191–1203.

Felix J.D., Elliot E.M. & Shaw S.L. 2012. Nitrogen isotopic composition of coal-fired power plant NO_x: influence of emission controls and implications for global emission inventories. *Environmental Science and Technology 46*, 3528–3535.

Førland E.J., Benestad R., Hanssen-Bauer I., Haugen J.E. & Skaugen T.E. 2011. Temperature and precipitation development at Svalbard 1900–2100. *Advances in Meteorology 2011*, article no. 893790, doi: 10.1155/2011/893790.

Forsström S., Ström J., Pedersen C.A., Isaksson E. & Gerland S. 2009. Elemental carbon distribution in Svalbard snow. *Journal of Geophysical Research—Atmospheres 114*, D19112, doi: 10.1029/2008JD011480.

Freyer H.D. 1991. Seasonal variation of $^{15}N/^{14}N$ ratios in atmospheric nitrate species. *Tellus B 43*, 30–44.

Freyer H.D., Kobel K., Delmas R.J., Kley D. & Legrand M.R. 1996. First results of $^{15}N/^{14}N$ ratios in nitrate from alpine and polar ice cores. *Tellus B 48*, 93–105.

Gibbons J.D. & Chakraborti S. 2003. *Nonparametric statistical inference*. 4th edn. Boca Raton, FL: CRC Press.

Goto-Azuma K. & Koerner R.M. 2001. Ice core studies of anthropogenic sulfate and nitrate trends in the Arctic. *Journal of Geophysical Research—Atmospheres 106*, 4959–4969.

Hastings M.G. 2010. Evaluating source, chemistry and climate change based upon the isotopic composition of nitrate in ice cores. *IOP Conference Series: Earth and Environmental Science 9*, article no. 012002, doi: 10.1088/1755-1315/9/1/012002.

Hastings M.G., Jarvis J.C. & Steig E.J. 2009. Anthropogenic impacts on nitrogen isotopes of ice-core nitrate. *Science 324*, 1288.

Hastings M.G., Steig E.J. & Sigman D.M. 2004. Seasonal variations in N and O isotopes of nitrate in snow at Summit, Greenland: implications for the study of nitrate in snow and ice cores. *Journal of Geophysical Research—Atmospheres 109*, D20306, doi: 10.1029/2004JD00499.

Heaton T.H.E. 1987. $^{15}N/^{14}N$ ratios pf nitrate and ammonium in rain at Pretoria, South Africa. *Atmospheric Environment 21*, 843–852.

Heaton T.H.E., Wynn P. & Tye A.M. 2004. Low $^{15}N/^{14}N$ ratios for nitrate in snow in the High Arctic (79°N). *Atmospheric Environment 38*, 5611–5621.

Hisdal V. 1998. *Svalbard nature and history*. Oslo: Norwegian Polar Institute.

Honrath R.E., Guo S., Peterson M.C., Dziobak M.P., Dibb J.E. & Arsenault M.A. 2000. Photochemical production of gas phase NO_x from ice crystal NO_3^-. *Journal of Geophysical Research—Atmospheres 105*, 24183–24190.

Honrath R.E., Peterson M.C., Guo S., Dibb J.E., Shepson P.B. & Campbell B. 1999. Evidence of NO_x production within or upon ice particles in the Greenland snowpack. *Geophysical Research Letters 26*, 695–698.

Jarvis J.C., Steig E.J., Hastings M.G. & Kunasek S.A. 2008. Influence of local photochemistry on isotopes of nitrate in Greenland snow. *Geophysical Research Letters 35*, L21804, doi: 10.1029/2008GL035551.

Kahl J.D.W., Martinez D.A., Kuhns H., Davidson C.I., Jaffrezo J.-L. & Harris J.M. 1997. Air mass trajectories to Summit, Greenland: a 44-year climatology and some episodic events. *Journal of Geophysical Research—Oceans 102*, 26861–26875.

Kaiser J., Hastings M.G., Houlton B.Z., Röckmann T. & Sigman D.M. 2007. Triple oxygen isotope analysis of nitrate using the denitrifier method and thermal decomposition of N_2O. *Analytical Chemistry 79*, 599–607.

Kang S., Qin D., Mayewski P. & Gjessing Y. 2001. Snow chemistry in Svalbard, Arctic. *Bulletin of Glaciological Research 18*, 9–13.

Kekonen T., Moore J.C., Mulvaney R., Isaksson E., Pohjola V. & van De Wal R.S.W. 2002. A 800 year record of nitrate from the Lomonosovfonna ice core, Svalbard. *Annals of Glaciology 35*, 261–265.

Kühnel R., Björkman M.P., Vega C.P., Hodson A., Isaksson E. & Ström J. 2013. Reactive nitrogen and sulphate wet deposition at Zeppelin Station, Ny-Ålesund, Svalbard. *Polar Research 32*, article no. 19136, doi: 10.3402/polar.v32i0.19136.

Kühnel R., Roberts T.J., Björkman M.P., Isaksson E., Aas W., Holmén K. & Ström J. 2011. 20-year climatology of NO_3^- and NH_4^+ wet deposition at Ny-Ålesund, Svalbard. *Advances in Meteorology 2011*, article no. 406508, doi: 10.1155/2011/406508.

Li D. & Wang X. 2008. Nitrogen isotopic signature of soil-released nitric oxide (NO) after fertilizer application. *Atmospheric Environment 42*, 4747–4754.

Liu S.C., Trainer M., Fehsenfeld F.C., Parrish D.D., Williams E.J., Fahey D.W., Hübler G. & Murphy P.C. 1987. Ozone production in the rural troposphere and the implications for regional and global ozone distributions. *Journal of Geophysical Research—Atmospheres 92*, 4191–4207.

Michalski G., Scott Z., Kabiling M. & Thiemens M.H. 2003. First measurements and modeling of $\Delta^{17}O$ in atmospheric nitrate. *Geophysical Research Letters 30*, article no. 1870, doi: 10.1029/2003GL017015.

Morin S., Erbland J., Savarino J., Domine F., Bock J., Friess U., Jacobi H.-W., Sihler H. & Martins J.M.F. 2012. An isotopic view on the connection between photolytic emissions of NO_x from the Arctic snowpack and its oxidation by reactive halogens. *Journal of Geophysical Research—Atmospheres 117*, D00R08, doi: 10.1029/2011JD016618.

Morin S., Savarino J., Bekki S., Gong S. & Bottenheim J.W. 2007. Signature of Arctic surface ozone depletion events in the isotope anomaly ($\Delta^{17}O$) of atmospheric nitrate. *Atmospheric Chemistry and Physics 7*, 1451–1469.

Morin S., Savarino J., Frey M.M., Domine F., Jacobi H.-W., Kaleschke L. & Martins J.M.F. 2009. Comprehensive isotopic composition of atmospheric nitrate in the Atlantic Ocean boundary layer from 65°S to 79°N. *Journal of Geophysical Research—Atmospheres 114*, D05303, doi: 10.1029/2008JD010696.

Morin S., Savarino J., Frey M.M., Yan N., Bekki S., Bottenheim J.W. & Martins J.M.F. 2008. Tracing the origin and fate of NO_x in the Arctic atmosphere using stable isotopes in nitrate. *Science 322*, 730–732.

Mosier A.R., Bleken M.A., Chaiwanakupt P., Ellis E.C., Freney J.R., Howarth R.B., Matson P.A., Minami K., Naylor R., Weeks K.N. & Zhu Z.-L. 2002. Policy implications of human-accelerated nitrogen cycling. *Biogeochemistry 57–58*, 477–516.

Nuth C., Kohler J., König M., von Deschwanden A., Hagen J.O., Kääb A., Moholdt G. & Pettersson R. 2013. Decadal changes from a multi-temporal glacier inventory of Svalbard. *The Cryosphere 7*, 1603–1621.

Pohjola V.A., Martma T.A., Meijer J.A.J., Moore J.C., Isaksson E., Vaikmäe R. & van de Wal R.S.W. 2002. Reconstruction of three centuries of annual accumulation rates based on the record of stable isotopes of water from Lomonosovfonna, Svalbard. *Annals of Glaciology 35*, 57–62.

Quinn P.K., Shaw G., Andrews E., Dutton E.G., Ruoho-Airola T. & Gong S.L. 2007. Arctic haze: current trends and knowledge gaps. *Tellus B 59*, 99–114.

Rasmussen L.A. & Kohler J. 2007. Mass balance of three Svalbard glaciers reconstructed back to 1948. *Polar Research 26*, 168–174.

Rinnan R., Michelsen A., Bååth E. & Jonasson S. 2007. Fifteen years of climate change manipulations alter soil microbial communities in a Subarctic heath ecosystem. *Global Change Biology 13*, 28–39.

Röthlisberger R., Hutterli M.A., Wolff E.W., Mulvaney R., Fischer H., Bigler M., Goto-Azuma K., Hansson M., Ruth U., Siggaard M.-L. & Steffensen J.P. 2002. Nitrate in Greenland and Antarctic ice cores: a detailed description of post-depositional processes. *Annals of Glaciology 35*, 209–216.

Ruggirello R.M., Hermanson M.H., Isaksson E., Teixeira C., Forsström S., Muir D.C.G., Pohjola V., van de Wal R. & Meijer H.A.J. 2010. Current use and legacy pesticide deposition to ice caps on Svalbard, Norway. *Journal of Geophysical Research—Atmospheres 115*, D18308, doi: 10.1029/2010JD014005.

Samyn D., Vega C. & Pohjola V.A. 2012. Nitrate and sulfate anthropogenic trends in the 20th century from five Svalbard ice cores. *Arctic, Antarctic, and Alpine Research 44*, 490–499.

Schuler T.V., Dunse T., Østby T.I. & Hagen J.O. 2013. Meteorological conditions on an Arctic ice cap—8 years of automatic weather station data from Austfonna, Svalbard. *International Journal of Climatology 34*, 2047–2058.

Semb A., Braekkan R. & Joranger E. 1984. Major ions in Spitsbergen snow samples. *Geophysical Research Letters 11*, 445–448.

Shaver G.R. & Chapin F.S. III. 1980. Response to fertilization by various plant growth forms in an Alaskan tundra: nutrient accumulation and growth. *Ecology 61*, 662–675.

Stohl A., Berg T., Burkhart J.F., Fjæraa A.M., Forster C., Herber A., Hov Ø., Lunder C., McMillan W.W., Oltmans S., Shiobara M., Simpson D., Solberg S., Stebel K., Ström J., Tørseth K., Treffeisen R., Virkkunen K. & Yttri K.E. 2007. Arctic smoke–record high air pollution levels in the European Arctic due to agricultural fires in Eastern Europe in spring 2006. *Atmospheric Chemistry and Physics 7*, 511–534.

Twickler M. & Whitlow S. 1997. Appendix B. Guide for the collection and analysis of ITASE snow and firn samples. In P.A. Mayewski & I.D. Goodwin (compilers): *International Trans-Antarctic Scientific Expedition*: *200 years of past Antarctic climate and environmental change. Science and implementation plan, 1996: report from the ITASE Workshop, Cambridge, United Kingdom, 2–3 August, 1996*. Bern: Past Global Changes.

Vega C.P., Pohjola V.A., Samyn D., Pettersson R., Isaksson E., Björkman M.P., Martma T., Marca A. & Kaiser J. 2015. First ice core records of nitrate NO_3^- stable isotopes from Lomonosovfonna, Svalbard. *Journal of Geophysical Research—Atmospheres 120*, 313–330, doi: 10.1002/2013JD020930.

Wolff E.W. 1995. Nitrate in polar ice. In R. Delmas (ed.): *Ice core studies of global biogeochemical cycles*. Pp. 195–224. New York: Springer.

Xu L. & Penner J.E. 2012. Global simulations of nitrate and ammonium aerosols and their radiative effects. *Atmospheric Chemistry and Physics 12*, 9479–9504.